Aerosol Science and Technology, 41:828–839, 2007

ISSN: 0278-6826 print / 1521-7388 online
DOI: 10.1080/02786820701496587

Demonstration of a VUV Lamp Photoionization Source for Improved Organic Speciation in an Aerosol Mass Spectrometer

M. J. Northway,[1] J. T. Jayne,[1] D. W. Toohey,[2] M. R. Canagaratna,[1] A. Trimborn,[1] K.-I. Akiyama,[3] A. Shimono,[4] J. L. Jimenez,[5,6] P. F. DeCarlo,[2,6] K. R. Wilson,[7] and D. R. Worsnop[1]

[1]*Aerodyne Research, Inc., Billerica, Massachusetts, USA*
[2]*Department of Atmospheric and Oceanic Sciences, University of Colorado, Boulder, Colorado, USA*
[3]*Japan Automobile Research Institute, Ibariki, Japan*
[4]*Sanyu Plant Service Co., Ltd., Kanagawa-ken, Japan*
[5]*Department of Chemistry and Biochemistry, University of Colorado, Boulder, Colorado, USA*
[6]*Cooperative Institute for Research in the Environmental Sciences (CIRES), University of Colorado, Boulder, Colorado, USA*
[7]*Chemical Sciences Division, Lawrence Berkeley National Laboratory, Berkeley, California, USA*

In recent years, the Aerodyne Aerosol Mass Spectrometer (AMS) has become a widely used tool for determining aerosol size distributions and chemical composition for non-refractory inorganic and organic aerosols. All AMSs to date have used a combination of flash thermal vaporization and 70 eV electron impact (EI) ionization. However, EI causes extensive fragmentation and mass spectra of organic aerosols are difficult to deconvolve because they are composites of the overlapping fragmentation patterns of a multitude of species. In this manuscript we present an approach to gain more information about organic aerosol composition by employing the softer technique of vacuum ultraviolet (VUV) ionization in a Time-of-Flight AMS (ToF-AMS). Our novel design allows for alternation between photoionization (PI) and EI within the same instrument on a timescale of minutes. Thus, the EI-based quantification capability of the AMS is retained while improved spectral interpretation is made possible by combined analysis of the complementary VUV and EI spectra. PI and EI spectra are compared for several compounds and mixtures in multiple dimensions including size distributions and size-segregated mass spectra. In general, VUV spectra contain much less fragmentation than EI spectra and for many compounds the parent ion is the base peak in the VUV spectrum. Results for oleic acid are compared to experiments conducted using tunable VUV radiation from a synchrotron source and were shown to be comparable under similar conditions of photon energy and vaporizer temperature. Future technical modifications for improvements in sensitivity and its potential for ambient measurements will be discussed.

INTRODUCTION

Atmospheric aerosols are well known to affect human health, visibility, ecosystems and agriculture, and climate (Dockery et al. 1997; Watson 2002; NAPAP 1991; IPCC 2001). Organic aerosols compose up to 50% of all fine particulate matter below 2.5 μm in diameter ($PM_{2.5}$) in urban areas, and under many circumstances organic material may account for the majority of the ambient aerosol mass (Kanakidou et al. 2005). It is now widely surmised that organic aerosols contain hundreds to thousands of organic compounds in many chemical classes including alkanes, aldehydes, aromatics, acids, and oligomers (Kalberer et al. 2004; Hamilton et al. 2004). Of this organic aerosol mass, only a small fraction has been compositionally resolved, and much of the organic aerosol mass remains uncharacterized to this date. This lack of knowledge represents an important uncertainty in the role of anthropogenic activities on the future climate and on human health effects, and requires new approaches for the analysis of organic compounds (Murphy 2005).

Aerosol mass spectrometry is a growing area of focus for aerosol speciation because of the wealth of information it can provide on a wide variety of chemical classes in real time.

Received 27 November 2006; accepted 6 June 2007.

The authors wish to thank Silke Hings and Frank Drewnick, and Jose Jimenez's research group for help with ToF-AMS software analysis, and Dr. Tom Baer for useful discussions. Financial support for ARI was provided by two grants from the Department of Energy (DOE) SBIR program (Phase 1 and 2). Part of this work was supported by the Director, Office of Energy Research, Office of Basic Sciences, Chemical Sciences Division of the U.S. Department of Energy under contract No. DE-AC02-05CH11231. PFD and JLJ thank NCAR/UCAR grant 505-39607 and NSF CAREER grant ATM-0449815 for funding for data acquisition software development.

Address correspondence to Megan J. Northway, 45 Manning Rd., Billerica 01821, MA, USA. E-mail: mnorthway@aerodyne.com

Aerosol mass spectrometers generally detect particles through either a single-step particle vaporization/ionization process (laser ablation) (Murphy and Thomson 1995; Noble and Prather 2000; Hinz et al. 1996), or a two-step vaporization/ionization process using a combination of laser desorption/thermal vaporization and various ion detection methods (Jayne et al. 2000; Woods III et al. 2001). The mass spectra of ambient aerosol (particularly organic aerosol) obtained with these instruments are generally complex due to the extensive fragmentation caused by the high-energy ionization methods used.

The Aerodyne Aerosol Mass Spectrometer (AMS) is widely used for obtaining both quantitative chemical composition and size information for aerosols in real-time with no need for preconcentration of samples (Jayne et al. 2000; Canagaratna et al. 2006). The standard AMS uses a combination of flash vaporization, electron impact ionization, and either quadrupole or time-of-flight mass spectrometry to detect fragment ions of the non-refractory component of aerosol particles. Since 70 eV electron impact is universal and inherently linear, its use within the AMS provides quantification and broad detection capabilities. A drawback of the combined flash vaporization and EI ionization detection scheme of the AMS is that it results in extensive fragmentation of organic molecules and limits its organic speciation capability. A deconvolution technique has been developed recently to estimate the mass concentrations and size distributions of hydrocarbon-like and oxygenated organic aerosols in ambient air using an iterative custom principal component analysis method where the time series of m/z 57 and 44 are used as "first order" tracers for fresh "hydrocarbon-like" and oxygenated organic aerosols, respectively (Zhang et al. 2005). Further refinements of this method using the Positive Matrix Factorization (PMF) method offer promise for extracting a few more components from AMS EI data. Since organic aerosols consist of hundreds to thousands of individual chemical species, however, more specific information about the organic species in the aerosol is of great interest.

Less energetic, soft ionization methods, such as single photon ionization (SPI) with VUV light have been shown to simplify the complexity of organic mass spectra in both gas-phase and aerosol phase mixtures (Sykes et al. 2002; Öktem et al. 2004; Mühlberger et al. 2002; Butcher et al. 1999). Resonance-enhanced multi photon ionization (REMPI) is a related soft ionization technique that is highly sensitive, but generally suitable only for (UV absorbing) aromatic components of organic aerosols (Heger et al. 1999; Mühlberger et al. 2001; Cao et al. 2003). Single photon ionization is a more quantitative and linear technique and therefore is more promising for the analysis of gaseous species from the thermal vaporization of aerosol beams. The use of relatively bulky and complex laser systems for the production of pulsed VUV light, in many of these experiments, however, complicates the deployment of such instruments in the field.

Recently, several new sources of VUV radiation have been developed as alternatives to lasers. Low-pressure lamps filled with noble gases and excited by microwave or radio frequency discharge, provide a simple means for a stable, continuous source of VUV photons that may be used to ionize a vapor plume of organic molecules. Nearly all of the organic compounds have ionization energy bands lying within the energy range 8–11 eV, making rare gas lamps ideal light sources for detection of organic molecules (Butcher et al. 1999). In recent mass spectrometry studies, lamp sources with photon intensities on the order of 10^{13}–10^{14} photons sec^{-1} have been reported (Hanold et al. 2004; Kurabuyashi et al. 2005). In other studies, a rare gas lamp pumped with electrons was used to provide a focused source of VUV photons at the excimer emission lines (Mühlberger et al. 2005a, 2005b). Most recently, this lamp was used to examine urban aerosol species desorbed from a filter using a combination of thermal pyrolysis and photoionization time-of-flight mass spectrometry (Streibel et al. 2006).

In this manuscript we characterize a developmental VUV lamp-based photoionization module that can be used together with electron impact (EI) ionization within an Aerodyne Aerosol Mass Spectrometer to provide improved analysis of organic components. We present our experimental design of a compact, robust field-deployable VUV module that is compatible with the current AMS and the first results from the technique. The complementary information provided by the EI and photoionization (PI) spectra for both bulk aerosol and size-segregated aerosol is illustrated for a number of pure and mixed organic aerosol particles. Lastly, the results from the VUV module are closely compared to similar experiments conducted using the tunable VUV radiation at the Advanced Light Source in Berkeley, California. The sensitivities and limits of detection of this method and its potential application for real-time organic aerosol analysis are discussed.

EXPERIMENTAL SECTION

1. ToF-AMS

The Aerodyne Aerosol Mass Spectrometer (AMS) has been described in detail elsewhere (Jayne et al. 2000; Canagaratana et al. 2006). For this study the newly developed time-of-flight (TOF) version of the AMS (referred to as the ToF-AMS) was used, where the traditional quadrupole mass spectrometer has been replaced by a compact orthogonal extraction time-of-flight mass spectrometer (Tofwerk AG, Thun, Switzerland) (Drewnick et al. 2005). The ToF-AMS instrument and the high-resolution version of the same instrument have been described previously (DeCarlo et al. 2006); hence, only the relevant details are described here.

As in the case of the quadrupole AMS, aerosol particles are sampled into the ToF-AMS using an aerodynamic lens (Zhang et al. 2002). The particles exit the lens and pass through a 1 mm i.d. channel skimmer, which skims most of the remaining air and transmits the particle beam into the aerosol-sizing chamber (pressure $\sim 1 \times 10^{-5}$ Torr). In this expansion, the particles achieve a terminal velocity depending on their vacuum

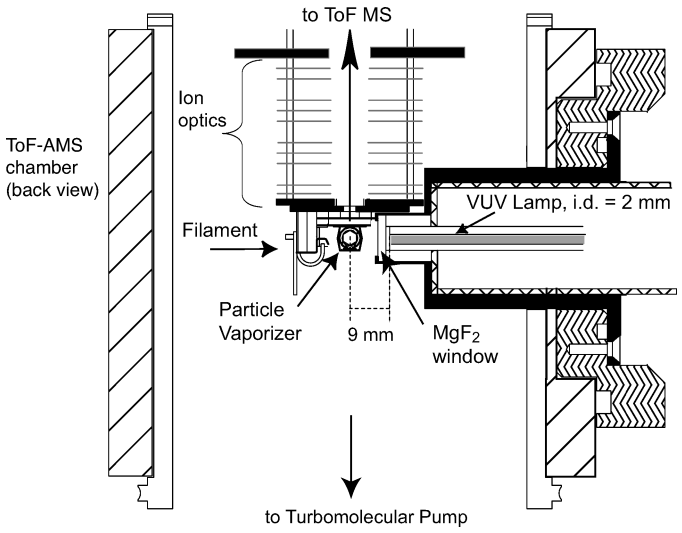

FIG. 1. Cross-sectional view of the VUV module and ionization region of the Aerodyne ToF-AMS. The particle beam is coming into the page.

aerodynamic diameters (DeCarlo et al. 2004). The particle beam next encounters a rotating mechanical chopper (chopper cycle, 150 Hz, effective duty cycle 2%) that produces pulses of particles, the phasing of which is used to determine particle diameters based on variable particle flight times. After the particles travel through the aerosol sizing chamber they impact on a heated tungsten vaporizer ($\sim$600°C) and all non-refractory components of the aerosol vaporize. As the particle is rapidly vaporized, the vapor plume is immediately ionized via electron impact with 70 eV electrons emitted by a tungsten filament.

Ions are extracted into the ToF-AMS with a pulse rate of 83.3 kHz, over a variable mass range from 1 to 1000 amu. When using a mass range of 0 to 300 amu, acquisition of one mass spectrum takes less than 12 μsec. As this time scale is much less than that of a chopper cycle (150 Hz), multiple mass spectra are obtained for each particle size, and even mass spectra of individual particles are possible. At these conditions and including the necessary dead times in the data acquisition system, typically about 500 spectra are taken for each chopper cycle. Ions are detected with a chevron-style multi-channel plate (MCP) detector (Burle Technologies, Sturbridge, MA). An important feature of the ToF-AMS is the high-speed (1Gs/s) analog-to-digital converter data card (AP240, Acqiris, Geneva, Switzerland). This board allows for the averaging of raw mass spectra in real time before transfer to a PC for storage. In addition, the AP240 allows for the user to input a noise "threshold" below which all data are discarded. The threshold is set above the electronic noise level, but below the average signal peak height for a single ion. This allows for discrimination of ions as single events, and their temporal distributions reflects Poisson ion counting statistics. Because of the relatively low signals in the VUV ionization mode in comparison to the electron impact mode, this discrimination is critical for the improving the signal-to-noise levels and results in the adequate signals in minutes.

2. VUV Ionization Module

A cross section of the modified AMS ionization region is shown in Figure 1. In the typical AMS systems only one filament is run at a time, but two filaments are present to avoid the need to vent the instrument if the filament in use fails. To operate in VUV mode, one of the two filaments is removed and replaced with the VUV lamp assembly. The assembly, consisting of an adapter flange, a stainless steel/window housing, and a module containing the VUV lamp and associated electronics, mounts to an existing port on the vacuum chamber, allowing for direct access to the ionization region. The entire assembly weighs about 3 kg with dimensions of 20 mm $\times$ 10 mm $\times$ 8 mm. The stainless steel window housing contains an MgF_2 window (TMS Vacuum Components, East Sussex, England) such that the lamp is operated at atmospheric pressure, but the VUV photons are transmitted through the MgF_2 into the high vacuum of the ionization region. The lamp itself is custom made by filling a quartz tube with $\sim$1–3 Torr of Krypton gas and a chemical getter (Barium metal) and sealing it with an MgF_2 window. During operation, a low flow of N_2 is continually introduced to purge any space between the two MgF_2 windows and avoid absorption of the VUV light from atmospheric oxygen. The VUV light is initiated by a high voltage discharged and maintained by a solenoidally coupled 180-MHz radiofrequency discharge powered by a $\sim$5–10 W single-stage oscillator/amplifier.

Figure 2 shows a typical spectrum of a VUV lamp, with two strong emission lines at 10 and 10.6 eV, (123.6 nm and 118.0 nm, respectively). These wavelengths are emitted as a result of the decay of collisionally excited Kr atoms created by the RF-discharge. Each lamp is about 5 cm long with an o.d. of 6 mm and an i.d. of 2 or 3 mm. Thus, the useful portion of the plasma is contained within the small volume adjacent to the window. The photon intensity at the exit of the Krypton lamp of the VUV module is estimated to be 5×10^{13} photons sec^{-1}. This

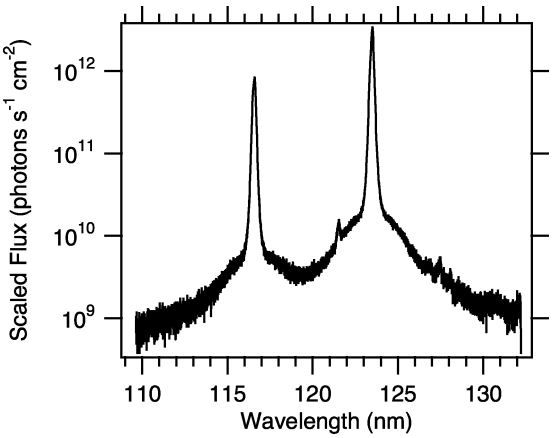

FIG. 2. VUV spectrum of a typical Krypton lamp used here, showing the two atomic line emissions at 116.5 nm (10.6 eV) and 123.6 nm (10 eV).

estimate, which is likely only accurate within a factor of 4, was obtained by exposing a phototube (Hamamatsu, Shizuoka-ken, Japan) to the lamp and measuring its direct current output after amplification with an analog current amplifier. The average photocathode activity over the entire surface specified by the manufacturer (12 mA/Watt at 121.6 nm) was used in the estimation. Using this value and the active area of the plasma, the total flux at the immediate lamp exit was calculated to be 5×10^{14} photons sec^{-1} cm^2. The absolute values shown in Figure 2 have been scaled to reflect this total flux value.

As shown in Figure 1, when the VUV module is connected to the ToF-AMS, the photons enter the ionizer through a 3 mm diameter aperture on its side. The light lost due to this baffling was simulated by placing a 3 mm mask in front of the phototube. From these experiments it was estimated that the VUV beam divergence is about 2 mm per 10 mm (~0.10 steradians), resulting in a light output at the exit of the lamp of 5×10^{14} photons sec^{-1} $steradian^{-1}$. This lamp brightness is similar to those quoted for commercially available VUV lamps with similarly sized plasma volumes. Including both the $1/r^2$ losses and the baffling effect, the total number of photons reaching the ionizer is estimated to be about 2×10^{13} photons sec^{-1}. For reference about 1.5×10^{16} electrons (2.5 mA) are emitted from the filament in the EI AMS.

3. Aerosol Generation

Laboratory aerosols were generated one of two ways. The first method was to dissolve a small amount of sample in a solvent and use a constant output collision atomizer (TSI Inc. Model 3076, St. Paul, MN) to generate a polydisperse sample of pure aerosol with a size mode between 10–1000 nm with a peak at ~100 nm. Pristane was dissolved in dichloromethane, atomized, and dried through a tube filled with activated charcoal. The second method, used generally for oleic acid, was to nucleate aerosols homogeneously by heating a bath of the pure compound and subsequently creating a supersaturation by cooling the air. The cigarette smoke aerosol was sampled in the laboratory as a sidestream measurement with the AMS inlet. This mixture was sampled "in situ" with no pre-concentration.

4. Synchrotron Measurements

To further characterize the VUV photoionization module, a number of experiments were conducted with the AMS at the Chemical Dynamics Beamline of the Advanced Light Source (ALS) at the Lawrence Berkeley National Laboratory. The synchrotron VUV light is generated from an undulator and can be continuously tuned from 7 to 25 eV. The source delivered a highly polarized photon beam of $\sim 10^{16}$ photons sec^{-1} with a spot size of approximately 1 mm (horizontal) by 0.2 mm vertical directly into the ionization region of the AMS. The AMS was coupled to the light source using a similar set-up to that shown in Figure 1, where the light beam entered the ionization region of the AMS through a vacuum flange on the side of the instrument. The alignment of the beam in the AMS ionizer was carefully tuned by both visual alignment using a window and by minute adjustments of the position of the instrument relative to the photon beam.

RESULTS AND DISCUSSION

1. Comparisons of EI and PI spectra

Figure 3 shows a comparison of electron impact and photoionization mass spectra for pristane (IUPAC name = 2,6,10,14-tetramethylpentadecane). Pristane is a simple, highly branched alkane, which is representative of a hydrocarbon-like mass spectrum with a high fraction of small alkyl fragments. The spectrum in Figure 3a highlights the extensive fragmentation that is typically observed in AMS EI spectra for this type of organic species. The EI spectrum is dominated by ions that result from secondary fragmentation of the primary ion fragments (m/z 113, m/z 183, and m/z 253) of pristane (McLafferty and Turecek 1993). These secondary ions, at m/z 43, 57, and 71, are commonly observed ions for EI spectra of alkanes. The molecular ion at m/z 268 is not visible on a linear scale in the EI spectrum. Although the PI spectrum also contains the ions at m/z 43, 57, and 71, it shows clearly the primary fragments and a prominent peak at the pristane molecular ion on a linear scale. Thus, the PI spectrum provides more specific information about the pristane parent molecule than the EI spectrum.

Figure 4 shows EI and PI spectra for cigarette smoke, which is a rich mixture of unsaturated aliphatic hydrocarbons, carboxylic acids, PAHs, and oxygen and nitrogen heterocyclic aromatic compounds (Rogge et al. 1994). Overall, the photoionization spectrum differs from the EI spectrum in that it contains many high mass fragments above m/z 100 that are visible on the linear scale, including some above m/z 400. Previous studies of cigarette smoke particles reported that although nicotine is a fairly volatile compound, it is an abundant compound found in cigarette smoke particles (Rogge et al.

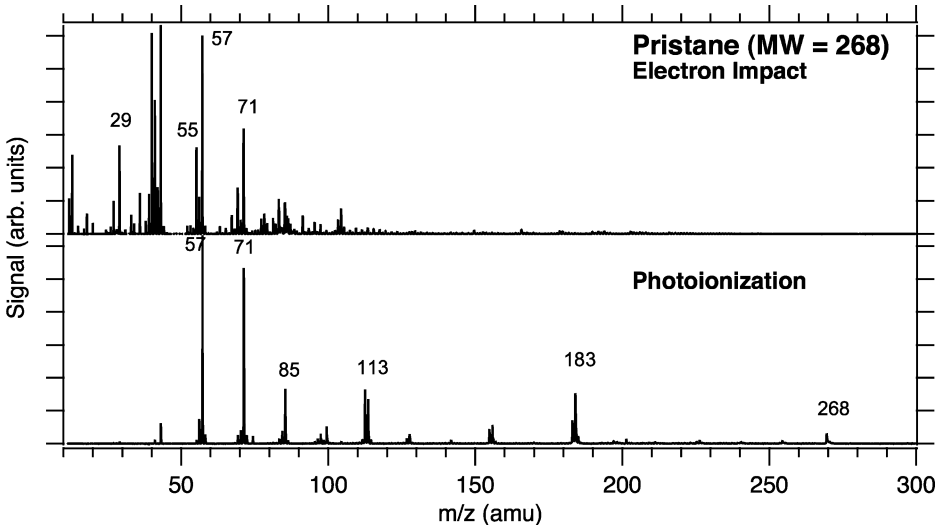

FIG. 3. Comparison of ionization techniques for pristane particles.

1994). The molecular mass of nicotine, m/z 162, is a prevalent peak in the PI spectrum, but not in the EI spectrum. The m/z 84 fragment ion, which dominates the PI spectrum and is present in the EI spectrum, corresponds to another nicotine fragment (NIST 2005). Although there is signal at almost every peak out to about m/z 400, many of the most dominant peaks are found to be consistent with organic molecules identified in GC/MS studies on cigarette particles that make up approximately 27% of the measured organic mass (Rogge et al. 1994). The peaks at m/z values 95 and 146, for example, may correspond to the molecular ions of 3-hydroxypyridine and myosmine which are two heterocyclic nitrogen-containing compounds generally found in large amounts in cigarette smoke particles. The large peak at m/z value 110 could similarly result from the molecular ion of any of the dihydroxybenzenes such as 1,2-dihydroxybenzene (catecol), 1,3-dihydroxybenzene (resorcinol) or 1,4-dihydroxybenzene (hydroquinone) (Pers. Comm. A. Shimono; Rogge et al. 1994). Similarly, the peak at m/z 124 may result from 3- or 4-methyl catecol, which are noted carcinogens also present in side stream measurements (Pers. Comm. A. Shimono). The hydrocarbon series of high mass peaks at m/z values 380, 394, 408, 422, and 436 is consistent with long chain hydrocarbons (C27-C31), which have been found in high loadings in cigarette smoke. The peaks at m/z 178 and m/z 202 are indicative of PAH species anthracene/phenanthrene and pyrene/fluoranthene respectively. Since the PAHs are typically resistant to fragmentation, they are observed as parent ions in both the EI and PI spectra. Because cigarette smoke is such a rich mixture of hundreds of compounds, these peak assignments are tentative, but this type of analysis illustrates the way in which

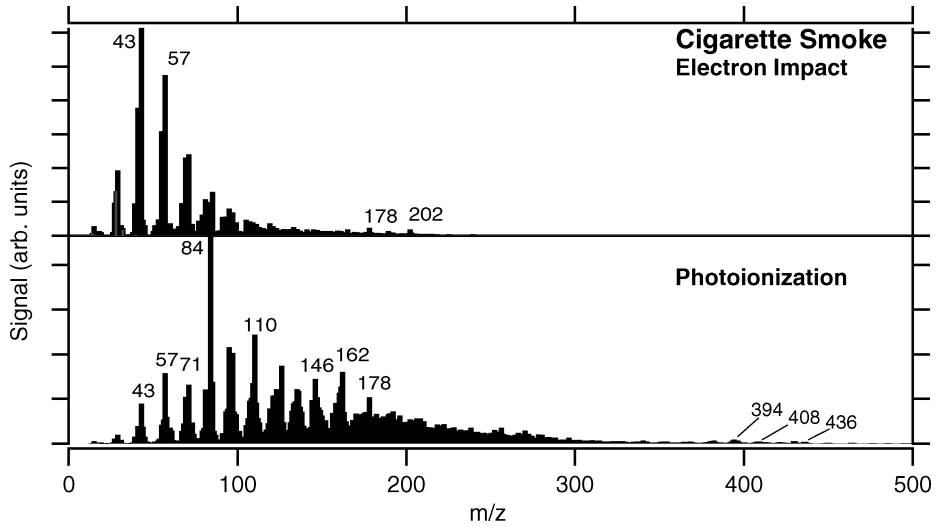

FIG. 4. Comparison of electron impact and VUV ionization mass spectra for cigarette smoke.

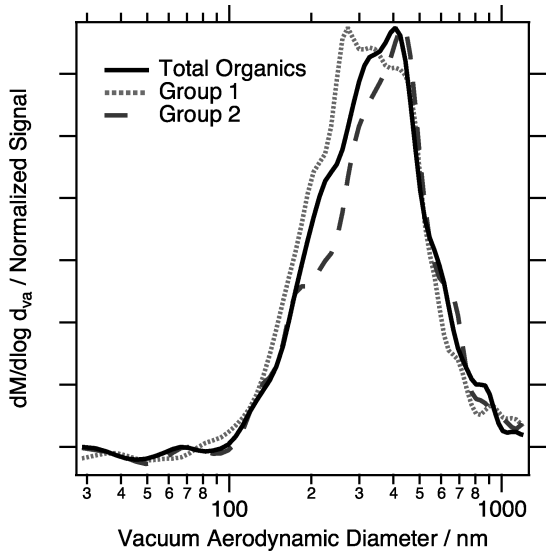

FIG. 5. VUV photoionization normalized size distributions from cigarette data for total organics (black line) and the weighted average of selected m/z values (tentative compound assignments from text in parentheses) for Group 1 (gray dotted line): 110 (dihydroxybenzenes) and 146 (myosmine), and Group 2 (dark gray dashed line): m/z 84 (nicotine fragment), 95 (hydroxypyridine), 162 (nicotine), and 178 (anthracene/phenanthrene).

PI spectra can enhance the chemical speciation capability of the AMS.

Links between aerosol chemical composition and aerosol size can be used to obtain even more detailed information about organic aerosol sources and processes in the atmosphere. For example, in previous studies chemically speciated size distributions have been used in quadrupole-based AMS studies to differentiate between fresh combustion aerosols and aged oxidized organic aerosols (Alfarra et al. 2004; Jayne et al. 2000). The ToF-AMS, with either EI or PI ionization, is also capable of providing chemically resolved particle size distributions. Figure 5 shows the average size dependent distribution for the total organic mass and two groups of PI fragments measured while sampling cigarette smoke particles. Group 1 consists of m/z 110 and 146 (likely from any of the dihydroxybenzenes and myosmine, respectively) which peak at around 250 nm. Group 2 consists of nicotine fragments (m/z 162 and 84) and other m/z values that are tentatively assigned to hydroxypyridine (m/z 95) and anthracene/phenanthrene (m/z 178). The latter size distribution peaks near 450 nm. The different size distributions for the two groups of organic ions and fragments clearly indicate that the size distribution observed for the total organic mass has contributions from overlapping modes of different composition.

Since the ToF-AMS instrument provides a complete EI and PI mass spectrum for every size bin, the size dependence of the cigarette smoke particle composition can be examined in more detail. This is demonstrated in Figure 6 which shows PI mass spectra averaged over the size bins 20–350 nm, 350–600 nm, and 600–1200 nm from Figure 5. The PI mass spectra clearly show differences in the aerosol chemical composition with particle size. The smallest size mode is dominated by the m/z value 110, but the middle and largest size modes are dominated by the nicotine fragment (m/z 84), as in the total mass spectrum (Figure 4). The relative importance of the m/z 178 (possibly PAH) also decreases as size increases. As illustrated in Figure 4, PI fragments at high m/z contain significant molecular information; hence, they provide more useful and relevant information about the size dependence of aerosol composition than the chemically-speciated size distributions measured with EI alone. Thus, the combination of PI with chemically resolved size distributions from the ToF-AMS promises to be a powerful tool for examining size-dependent chemical variations in aerosol composition.

2. Optimizing Spectral Information Available with PI

The exact photoionization spectrum (i.e., degree of fragmentation) from a particular compound depends strongly on both the sample temperature (aerosol vaporization method) and the photoionization energy used. Both of these factors can contribute excess energy to the ions and may result in additional fragmentation of the molecular ion. Previous studies have shown that the degree of fragmentation can be reduced by using lower vaporization temperatures or by using lower photon energies (Nash et al. 2005; Wilson et al. 2005; Mysak et al. 2005). For example, for the compound oleic acid, researchers have obtained VUV spectra with very little fragmentation (Mysak et al. 2005). In order to study the exact fragmentation observed using our system, spectra of oleic acid were taken under a number of varying conditions. Figures 7a and 7b show the EI and PI spectra for oleic acid taken with the vaporizer at 500°C, standard operating conditions for EI. Since oleic acid has a backbone that consists of a long chain alkane, its EI spectrum has many secondary fragments that are the same as in the pristane spectrum (Figure 3). The PI spectrum of oleic acid, on the other hand, shows significant differences not only from the oleic acid EI spectrum but also from the pristane PI spectrum. Figure 7c shows the same photoionization spectrum of oleic acid particles taken with the AMS vaporizer temperature at 200°C. When compared to Figure 7b, it is clear that the extent of fragmentation is highly dependent on the internal energy of the molecules prior to ionization. In Figure 7c, relative to the molecular ion (m/z 282) the intensity of the fragment ions (particularly at m/z 84, 98, and 111) has decreased with decreased AMS vaporizer temperature, and the m/z 264 is now the highest peak in the spectrum. The ion fragment at m/z 264 results from the loss of the water ion from the parent ion, likely from thermal decomposition of the molecule upon vaporization and not from a ion fragmentation process, and is thus a surrogate for the molecular ion of oleic acid. Thus, it may be inferred that a significant amount of fragmentation can be avoided by using vaporizer temperatures just above the boiling point (or thermal decomposition point) of the compounds of interest. However, in most cases, such as in sampling atmospheric aerosol, there will be many organic compounds present in the aerosol, and

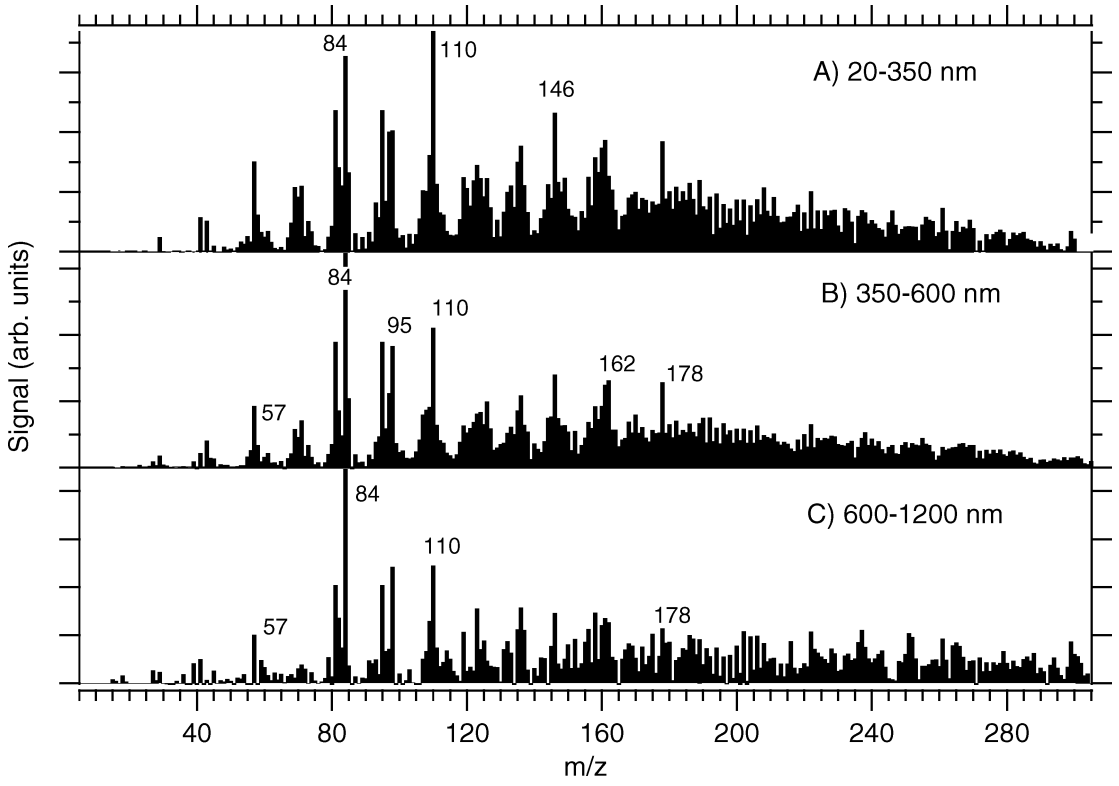

FIG. 6. Size-segregated mass spectra for the cigarette smoke particles shown in Figures 4 and 5. Size bins are labeled as (a) 20–350 nm, (b) 350–600 nm, and (c) 600–1200 nm.

therefore optimizing the temperature for minimal fragmentation for all compounds is not possible.

One complication that arises when acquiring PI spectra is unintended electron impact ionization that results from photoelectrons that are formed in the ionization region (Mühlberger et al. 2005a). Photoelectrons are produced in the ionization region by photons striking the metal surfaces of the ionizer. As they are typically formed, these photoelectrons have sufficient energy to ionize the air, water, and oxygen molecules (ionization energies of 12–14 eV) that are present as gas phase molecules in the focused molecular beam but are not photoionized by 10.6 eV VUV photons. Thus, the presence of these signals is indicative of photoelectron impact occurring in the ionization region. When aerosol signals are small ($<10\ \mu g\ m^{-3}$) these air peaks are sometimes the largest in the mass spectrum. When photoelectrons are present, electron impact ionization also occurs for vaporized aerosol molecules. For example, the presence of some inorganic aerosol signals in the ambient mass spectrum, such as ammonia and nitrate, is another indication of photoelectrons in the system. Moreover, for any given compound, the presence of photoelectrons will generally cause much more fragmentation of the molecular ion than in pure photoionization, causing the mass spectrum to look more like an electron impact spectrum.

The number of photoelectrons can be reduced by minimizing the metal surface area in the system that is exposed to stray and diverging photons from the lamp. We have attempted to do this in our system by positioning the lamp as close as possible to the ionization region of the AMS, thereby minimizing $1/r^2$ divergence of photons from the lamp. The improved design brought the lamp 5 mm closer to the ionizer and reduced the number of photoelectrons by an estimated factor of 20–50. This design also improved the photon delivery to the ionization region by a factor of 2, resulting in a corresponding increase in sensitivity. The N_2^+ and O_2^+ signals from photoelectrons were also reduced by a similar factor. Figures 7c and 7d show a comparison of the photoionization of oleic acid particles at 200°C using the initial and modified designs of the VUV module. Although the spectra are very similar above 150 amu, the spectrum from the new VUV interface design shows a dramatic decrease in the relative intensity of the fragment ions below m/z 100, indicating reduced electron impact. In particular the fragment ions at m/z 43, 55, and 69 seem to be mostly generated by electron impact and are much reduced ($\sim\times$20–50), which is consistent with the reduction in photoelectrons in the new design. In order to quantify the extent to which the electron impact ionization was reduced in the improved VUV module, the oleic acid spectra discussed above were compared with similar experiments carried out at the Advanced Light Source in Berkeley, CA. The synchrotron photon beam was delivered to the AMS in an analogous manner to the VUV lamp module in standard operation. However, because

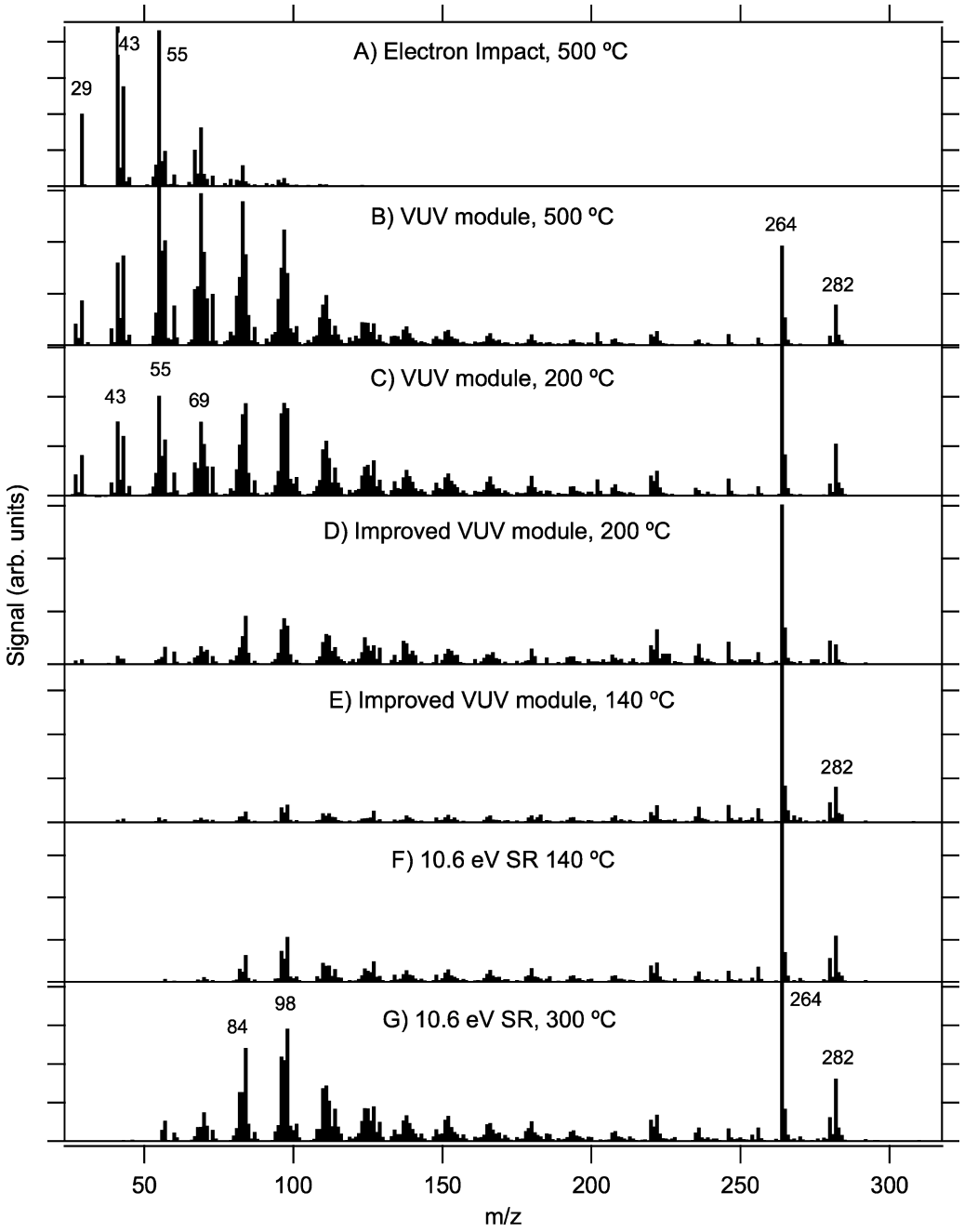

FIG. 7. Comparison of spectra of oleic acid aerosol taken at varying conditions: (a) EI spectrum with vaporizer at 500°C. (b) VUV module with vaporizer at 500°C. (c) VUV module with vaporizer at 200°C. (d) 200°C using improved VUV module (e) 140°C using improved VUV module. (f) 140°C using synchrotron radiation at 10.6 eV g) 300°C using synchrotron radiation at 10.6 eV.

the diameter of the synchrotron photon beam is much smaller than the entrance aperture into the AMS ionizer, the possibility of photoelectron production and electron impact contamination using this source was nearly zero. Figures 7e and 7f show the oleic acid spectrum using the improved VUV module and the synchrotron radiation at 10.6 eV both taken at an AMS vaporizer temperature of 140°C. Indeed a visual comparison of these two spectra shows a striking similarity, suggesting that most of the electron impact has been removed in the improved VUV module. Figure 7g shows the oleic acid PI spectrum taken using the synchrotron radiation at 10.6 eV at an AMS vaporizer temperature 300°C. Note that the fragmentation at 300°C (7g) using the pure photoionization from the SR is notably different from the fragmentation at 200°C using the old VUV module (7c),

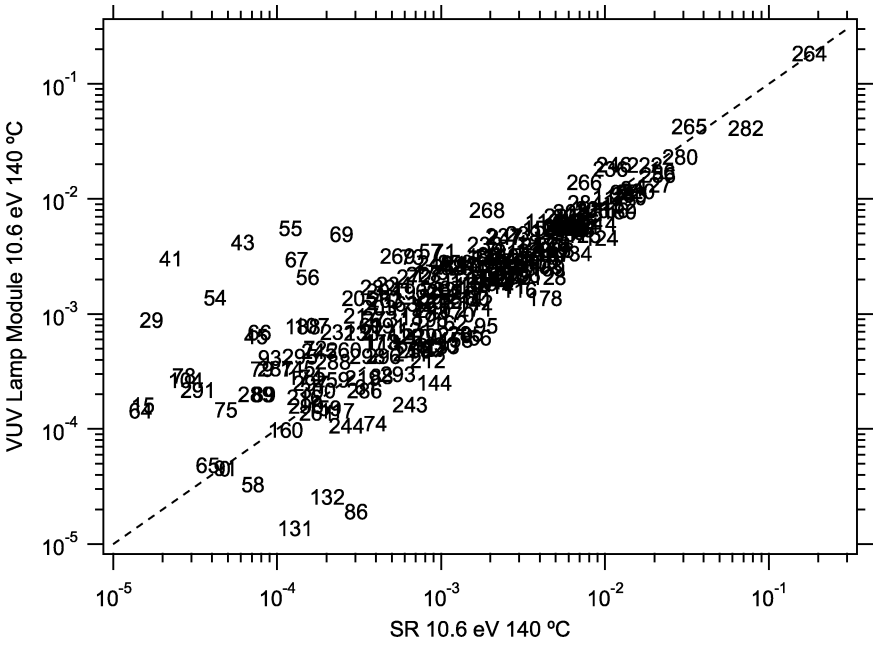

FIG. 8. Correlation plot comparing mass spectra taken using VUV lamp module (Figure 7e) and the synchrotron radiation (Figure 7f), both at 140°C.

providing evidence that much of the fragmentation in 7c is due to electron impact ionization and not excess thermal energy. In particular, the fragments at m/z 84 and 98 are increased from the excess thermal energy, but not those at m/z 43, 55, and 69. Finally, Figure 8 shows a scatter plot of the mass spectra from Figures 7e and 7f, indicating good agreement between the two spectra. The fragment ions that notably fall off the line, m/z 43, 55, and 69, are likely mostly due to the small amount of photoelectron impact ionization that still remains in our system. However, as shown in the normalized log plot, these fragments are less than 0.01% of the total signal, suggesting that the photoelectrons in our system have been reduced to a nearly negligible level.

Figure 9 shows the results of synchrotron experiments that mapped the PI spectra of oleic acid as a function of VUV energy and AMS vaporizer temperature. The ratio of the molecular ion and base peak sum (m/z 282 + m/z 264) to the total ion signal (designated M^+/Total Ion) is maximized for all temperatures near the ionization energy of 8.7 eV (Mysak et al. 2005). At this point and the lowest temperatures, more than 75% of the signal is in the parent ion signal. As expected, increased AMS vaporizer temperature causes an increase in fragmentation at all energies above the ionization energy. However, the value of M^+/Total Ion reaches a maximum for all profiles around 100°C. Below this temperature there is very little excess thermal energy, however near this temperature the total signal does begin to decrease and vaporization of the oleic acid aerosol is presumably no longer a "flash vaporization" process. Thus, for soft ionization in the AMS it is important to find an optimum temperature where all of particles are vaporized, but thermal fragmentation is still minimized.

3. Sensitivity and Limits of Detection

The ionization efficiency in the AMS with the EI or PI process can be expressed as:

$$IE = \sigma \cdot F \cdot \tau \cdot E \qquad [1]$$

where σ is the appropriate ionization cross-section of the molecule of interest, F is the ionizing photon or electron flux, τ is the residence time available for ionization, and E is the ion transmission and detection efficiency of the mass spectrometer.

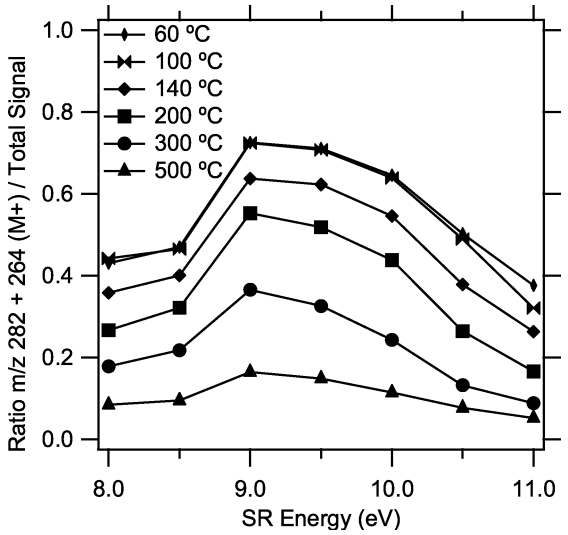

FIG. 9. Temperature and VUV photon energy dependence for photoionization of oleic acid using synchrotron radiation.

Thus, for a given mass spectrometer where τ and E do not vary, the relative IE for electron impact compared with photoionization can be expressed as:

$$IE_{EI}/IE_{PI} = (\sigma_{EI}/\sigma_{PI}) \cdot (F_{EI}/F_{PI}). \quad [2]$$

In general, for organic molecules the cross-sections for photoionization are 20–70 times smaller than the cross-sections for electron impact ionization (Cool et al. 2003; Berkowitz 2002; Jimenez et al. 2003). During EI ionization, the AMS ionizer usually operates at an emission current of 2.5 mA, which corresponds roughly to an output of 1.5×10^{16} electrons sec^{-1}. Since the evaporative plume produced by flash heating of a particle is confined by the ionizer geometry and is much smaller than the volume of light from the lamp (or electrons from the filament in the case of EI), the ionizing volume for both processes is assumed to be the same, and the value of F_{EI} /F_{PI} is approximately equal to the ratio of electron output to photon output for the two processes (units of photons sec^{-1} or electrons sec^{-1}). As discussed in the Experimental section, the VUV lamp yields an output of 2×10^{13} photons sec^{-1} at the ionizer, such that the value of F_{EI} /F_{PI} is 500. Thus taken together, according to equation 2, the IE_{EI}/IE_{PI} is estimated to be 1×10^4.

For the both the quadrupole and the ToF-AMS instruments IE_{EI} is routinely measured as a metric of the instrument sensitivity and stability (Jimenez et al. 2003). The calibration procedure involves the use of size-selected particles of known concentration. The IE is defined as the ratio of the average measured number of ions per particle to the known number of molecules per particle. The IE_{PI} has been measured by an analogous procedure for oleic acid. As summarized in Table 1, a typical measured value for IE_{EI} (for 70 eV electron impact) in a ToF-AMS for oleic acid is 1×10^{-6} and the measured IE_{PI} of oleic acid is 2×10^{-10}. The ratio of these measured values, 5000, is within a factor of 2 of the estimated value from Equation (2).

The detection limit in EI mode for organic species in a 1-minute average spectrum is approximately 20 ng m^{-3}(DeCarlo et al. 2006). Because the thresholding feature of the Acqiris data acquisition card can be used to discriminate against electronic noise, the instrument noise can be reduced to simply the dark counts of the MCP. For a new set of MCPs this value can be as low as 1 count per minute, although values of 2–5 counts per second are more typical. For the experiments here, the RMS noise calculated for the difference signal with no particles (filter measurement) is typically around 0.002 bits per extraction, which corresponds to 3 μg m^{-3} for a 1-minute average. Thus, the 3σ limit of detection for oleic acid is calculated to be about 12 μg m^{-3} for a 1-minute average, based on the measured ionization efficiency for this molecule shown in Table 1. This detection limit is ~1000 times, rather than 10,000 worse than for EI due to the ability to further discriminate against noise in the VUV mode by increasing the MCP gain. During EI operation the MCP gain is limited by avoidance of saturation of the large signals, which is not a concern for VUV operation. For some ions (e.g., m/z 43), there is a significant gas-phase background that increases the limit of detection for aerosol signals. Furthermore, at very high particle mass concentrations, ions scattered in the grids of the TOF flight region will arrive at m/z's other than their nominal values, resulting in baseline noise that also will affect the limits of detection. Limits of detection for many other organic molecules will generally be in the 10–12 μg range, depending on the specific photoionization cross section of the molecule. It should be noted that the limits of detection reported here are for a single component aerosol. Thus, the limit of detection must be exceeded for each compound in an aerosol mixture to detect a signal for that compound. This is in contrast to EI, where excessive fragmentation causes ions from different compounds to add, especially in the smaller m/z's, aiding in the detection of total organics.

TABLE 1
Comparison of EI and PI sensitivity parameters

	EI ionization	Photoionization (PI)	EI/PI
Flux, part cm^{-2} sec^{-1}	1×10^{16} /area	2×10^{13}/area	5×10^2
σ,cm^2 $molec^{-1}$	6×10^{-16}	3×10^{-17}	20
Measured IE	1×10^{-6}	2×10^{-10}	5×10^3
Predicted IE_{EI}/IE_{PI}			1×10^4

It is clear from Table 1 that the sensitivity of PI relative to EI can be improved by increasing the photon flux of the VUV lamp. The photon output of the lamp used in these studies is likely within a factor of 10 of its theoretical maximum for an unfocused beam. We believe that the plasma is near saturation for two reasons: first, when the input RF power is increased, the photon flux does not increase. Moreover, other commercially available lamps of the same geometry have similar outputs. For example, Resonance, Ltd, in Ontario, Canada, produces lamps with an output of 3×10^{15} photons $steradian^{-1}$ sec^{-1} for a 12 mm diameter lamp. The effective area of this lamp is 16 times larger than the 3 mm lamp used for the measurements shown in this manuscript, and therefore actually has a very similar output per area or flux as the lamp used here. Therefore, this lamp would not increase the sensitivity of method in the AMS without some way to concentrate the beam.

Other researchers have used different lamp designs to improve photon fluxes, without the use of a laser. Notably, Mühlberger and coworkers have developed the Electron-Beam-Pumped Excimer VUV lamp, whereby a Kr or Ar source is irradiated with electrons from an electron gun to create rare gas excimers (Mühlberger 2005a, 2005b). These excimers decay to produce VUV light that can be a source for single photon ionization. Reported photon intensities are presently about 1.5×10^{13} photons s^{-1}, but are expected to increase by a factor of ten in the near future (Mühlberger et al. 2005a). If indeed such

lamps eventually create more photons than the rare gas lamps of a similar size, they would allow for a sensitivity increase for VUV ionization within the AMS.

Another approach is to use the photons from the VUV lamp not for direct ionization but for the ejection of photoelectrons from a photoemissive surface that is coupled into the AMS. In this method, known as PERCI (Photoelectron Resonance Capture Ionization Mass Spectrometry), the photoelectrons are finely tuned to a low energy (<0.1 eV), by the addition of an extra electrode near the photoemissive surface (LaFranchi et al. 2004). These low energy photoelectrons attach to analyte molecules resulting in little or no fragmentation (LaFranchi et al. 2004). This technique could be a feasible alternative to photoionization in the AMS.

CONCLUSION

This manuscript presents the first results obtained from a field-deployable VUV lamp module that can be interfaced to the Aerodyne Aerosol Mass Spectrometer to provide PI spectra of aerosol chemical species in real time. The results presented here indicate that photoionization using rare gas lamps is a promising ionization technique for improving the molecular information provided by AMS mass spectra. Although the high temperature of the AMS vaporizer induces some thermal fragmentation, the PI spectra are less complex than EI spectra due to decreased fragmentation. The PI spectra obtained from the VUV lamp are similar to those obtained with VUV radiation from a synchrotron source. Comparisons of EI and PI spectra of pure organic aerosols show that the presence of parent peaks and characteristic fragments at masses greater than m/z 100 in the PI spectra provide clearer signatures for chemical identification. Even in more complex organic mixtures such as cigarette smoke particles, the PI spectra provide more information about the molecular composition of the aerosol than EI spectra. Speciated size distributions measured with the PI detection technique offer an additional means of increasing the chemical information that can be obtained by the AMS for complex mixtures of aerosol particles.

The reported PI detection limits of 10–12 μg m-3 in a 1-minute sample are sufficient for laboratory work, source sampling, and detection of atmospheric aerosol in polluted urban atmospheres at fixed sites. The PI spectra presented here, however, are limited by photon fluxes in comparison to electron fluxes in electron impact ionization, and span only 3–4 orders of magnitude in signal in comparison to the 7 orders of magnitude spanned by the current AMS in standard electron impact mode. With several ongoing advances in excimer rare gas lamp technology there is a significant potential of improving the sensitivity of the photoionization technique by a factor of 50–100, which would be similar to the existing quadrupole AMS instruments.

A key feature of the VUV lamp module design is its ability to alternate between PI and EI detection on the timescale of minutes. This feature allows for the combination of the advantages of both detection techniques. While PI offers spectral simplicity, alternation of PI with the EI allows for increased sensitivity to organic aerosol mass and maintains the AMS sensitivity to inorganic species like SO_4 and NO_3 which are not effectively ionized by 10.6 eV PI. The ability to alternate PI detection with EI is also important because electron impact ionization efficiency has an empirical dependence on chemical composition and molecular weight that can be readily used to quantify speciated mass.

REFERENCES

Alfarra, M. R., Coe, H., Allan, J. D., Bower, K. N., Boudries, H., Canagaratna, M. R., Jimenez, J. L., Jayne, J. T., Garforth, A. A., Li, S-M., and Worsnop, D. R. (2004). Characterization of Urban and Rural Organic Particulate in the Lower Fraser Valley using Two Aerodyne Aerosols Mass Spectrometers, *Atmos. Env.* 38:5745–5758.

Berkowitz, J. (2002). *Atomic and Molecular Photoabsorption: Absolute Total Cross Sections*. Academic Press, San Diego, 350 pp.

Butcher, D. J., Goeringer, D. E., and Hurst, G. B. (1999). Real-time Determination of Aromatics in Automobile Exhaust by Single-Photon Ionization Ion Trap Mass Spectrometry, *Anal. Chem.* 71:489–496.

Canagaratna, M. R., Jayne, J. T., Onasch, T. B., Williams, L. R., Trimborn, A., Northway, M. J., Kolb, C. E., Worsnop, D. R., Jimenez, J. L., Allan, J. D., Coe, H., Alfarra, M. R., Zhang, Q., Drewnick, F., and Davidovits, P. (2007). Chemical and Microphysical Characterization of Ambient Aerosols with the Aerodyne Aerosol Mass Spectrometer, *Mass Spectrom. Rev.* 26:185–222.

Cao, L., Mühlberger, F., Adam, T., Streibel, T., Wang, H. Z., Kettrup, A., and Zimmermann, R. (2003). *Anal. Chem.* 75:5639–5645.

Cool, T. A., Nakajima, K., Mostefaoui, T. A., Qi, F., McIlroy, A., Westmoreland, P. R., Law, M. E., Poisson, L., Peterka, D. S., and Ahmed, M. (2003). Selective Detection of Isomers with Photoionization Mass Spectrometry for Studies of Hydrocarbon Flame Chemistry. *J. Chem. Phys.* 119(16):8356–8365.

DeCarlo, P., Slowik, J. G., Worsnop, D. R., Davidovits, P., and Jimenez, J. L. (2004). Particle morphology and Density Characterization by Combined Mobility and Aerodynamic Diameter Measurements. Part 1: Theory. *Aerosol Sci. Technol.* 38:1185–1205.

DeCarlo, P. F., Kimmel, J. R., Trimborn, A., Northway, M., Jayne, J. T., Aiken, A. C., Gonin, M., Fuhrer, K., Hovarth, T., Docherty, K. S., Worsnop, D. R., and Jimenez, J. L. (2006). A Field-Deployable High-Resolution Time-of-Flight Aerosol Mass Spectrometer, *Anal. Chem,* 74:8281–8289.

Dockery, D. W., Pope, C. A., Xu, X. P., Spengler, J. D., Ware, J. H., Fay, M. E., Ferris, B. G., and Speizer, F. E. (1993). *New Engl. J. Med.* 329:1753–1759.

Drewnick, F., Hings, S. S., DeCarlo, P., Jayne, J. T., Gonin, M., Fuhrer, K., Weimer, S., Jimenez, J. L., Demerjian, K. L., Borrman, S., and Worsnop, D. R. (2005). A New Time-of-Flight Aerosol Mass Spectrometer (TOF-AMS)—Instrument Description and First Field Deployment. *Aerosol Sci. Technol.* 39:637–638.

Hamilton, J. F., Webb, P. J., Lewis, A. C., Hopkins, J. R., Smith, S., and Davy, P. (2004). Partially Oxidised Organic Components in Urban Aerosol using GCXGC-TOF/MS. *Atmos. Chem. Phys.* 4:1279–1290.

Hanold, K. A., Fischer, S. M., Cornia, H., Miller, C. E., and Syage, J. A. (2004). Atmospheric Pressure Photoionization. 1. General Properties for LC/MS. *Anal. Chem.* 76:2842–2851.

Heger, H. J., Zimmermann, R., Dorfner, R., Beckmann, M., Griebel, H., Kettrup, A., and Boesl, U. (1999). On-line Emission Analysis of Polycyclic Aromatic Hydrocarbons down to pptv Concentration Levels in the Flue Gas of an Incineration Pilot Plant with a Mobile Resonance-Enhanced Multiphoton Ionization Time-of-Flight Mass Spectrometer, *Anal. Chem.* 71:46–57.

Hinz, K.-P., Kaufmann, R., and Spengler, B. (1996). Simultaneous Detection of Positive and Negative Ions from Single Airborne Particles by Real-time Laser Mass Spectrometry. *Aerosol Sci. Technol.* 24:233–242.

Intergovernmental Panel of Climate Change (IPCC). (2001). *Climate Change 2001, The Scientific Basis*. Cambridge University Press, Cambridge, UK.

Jayne, J. T., Leard, D. C., Zhang, X., Davidovits, P., Smith, K. A., Kolb, C. E., and Worsnop, D. R. (2000). *Aerosol Sci. Technol*. 33:49–70.

Jimenez, J. L., Jayne, J. T., Shi, Q., Kolb, C. E., Worsnop, D. R., Yourshaw, I., Seinfeld, J. H., Flagan, R. C., Zhang, X., Smith, K. A., Morris, J. W., and Davidovits, P. (2003), Ambient Aerosol Sampling using the Aerodyne Aerosol Mass Spectrometer. *J. Geophys. Res*. 108(D7):8425.

Kalberer, M., Paulsen, D., Sax, M., Steinbacher, M., Dommen, J., Prevot, A., S. H., Fisseha, R., Weingartner, E., Frankevich, V., Zenobi, R., and Baltensperger, U. (2004). Identification of Polymers as Major Components of Atmospheric Organic Aerosols. *Science* 303:1659–1662.

Kanakidou, M, Seinfeld, J. H., Pandis, S. N., Barnes, I., Dentener, F. J., Facchini, M. C., Van Dingenen, R., Ervens, B., Nenes, A., Nielsen, C. J., Swietlicki, E., Putaud, J. P., Balkanski, Y., Fuzzi, S., Horth, J., Moortgat, G. K., Winterhalter, R., Myhre, C. E. L., Tsigaridis, K., Vignati, E., Stephanou, E. G., and Wilson, J. (2005). Organic Aerosol and Global Climate Modeling: A Review. *Atmos. Chem. Phys*. 5:1053–1123.

Kurabuyashi, S., Yamakoshi, H., Danno, M., Sakai, S., Tsuruga, S., Futami, H., and Morii, S. (2005). VUV Single-photon Ionization Ion Trap Time-of-Flight Mass Spectrometer for On-Line, Real-Time Monitoring of Chlorinated Organic Compounds in Waste Incineration Flue Gas, *Anal. Chem*. 77:1007–1012.

LaFranchi, B. W., Zahardis, J., and Petrucci, G. (2004). Photoelectron Resonance Capture Ionization Mass Spectrometry: A Soft Ionization Source for Mass Spectrometry of Particle-Phase Organic Compounds, *Rapid Commun. Mass Spectrom*. 18:2517–2521.

McLafferty, F. W., and Turecek, F. (1993). *Interpretation of Mass Spectra*. University Science Books, Sausalito, 371 pp.

Mühlberger, Wieser, J., A. Ulrich F., and Zimmermann, R. (2002). Single Photon Ionization (SPI) via Incoherent VUV-Excimer Light: Robust and Compact Time-of-Flight Mass Spectrometer for On-Line, Real-Time Process Gas Analysis, *Anal. Chem*. 74:3790–3801.

Mühlberger, F., Zimmermann, R., and Kettrup, A. (2001). A Mobile Mass Spectrometer for Comprehensive On-Line Analysis of Trace and Bulk Components of Complex Gas Mixtures: Parallel Application of the Laser-Based Ionization Methods VUV Single-Photon Ionization, Resonant Multiphoton Ionization, and Laser-Induced Electron Impact Ionization, *Anal. Chem*. 73:3590–3604.

Mühlberger, F., Wieser, J., Morozov, A., Ulrich, A., and Zimmerman, R. (2005). Single-Photon Ionization Quadrupole Mass Spectrometry with an Electron Beam Pumped Excimer Light Source, *Anal. Chem*. 77:2218–2226.

Mühlberger, F., Streibel, T., Wieser, J., Ulrich, A., and Zimmerman, R. (2005). Single photon Ionization Time-of-Flight Mass Spectrometer with a Pulsed Electron Beam Pumped Excimer VUV Lamp for On-Line Gas Analysis: Setup and first Results on Cigarette Smoke and Human Breath, *Anal. Chem*. 77:7408–7414.

Murphy, D. M. (2005). Something in the Air, *Science* 307:1888–1890.

Murphy, D. M., and Thomson, D. S. (1995). Laser Ionization Mass Spectroscopy of Single Aerosol Particles, *Aerosol Sci. Technol*. 22:237–249.

Mysak, E. R., Wilson, K. R., Jimenez-Cruz, M., Ahmed, M., and Baer, T. (2005). Synchrotron Radiation Based Aerosol Time-of-Flight Mass Spectrometer for Organic Constituents, *Anal. Chem*. 77:5953–5960.

Nash, D. G., Liu, X. F., Mysak, E. R., and Baer, T. (2005). Aerosol Particle Mass Spectrometry with Low Photon Energy Laser Ionization, *Int. J. Mass Spectrom*. 241:89–97.

National Acid Precipitation Assessment Program (NAPAP) (1991), 1990 Integrated Assessment Report. Washington DC, The US National Acid Precipitation Program, Office of the Director.

NIST Chemistry Webbook (2005), National Institute for Standards and Technology (NIST) Standard Reference Database, Number 69, Release June 2005. Available at: http://webbook.nist.gov/chemistry/.

Noble, C. A., and Prather, K. A. (2000). *Mass Spectrom. Rev.* 19:248.

Öktem, B., Tolocka, M. P., and Johnston, M. V. (2004). On-Line Analysis of Organic Components in Fine and Ultrafine Particles by Photoionization Aerosol Mass Spectrometer, *Anal. Chem*. 76:253–261.

Rogge, W. F., Hildemann, L. M., Mazurek, M. A., Cass, G. R., and Simonelt, B. R. T. (1994). Sources of Fine Organic Aerosol. 6. Cigarette smoke in the urban atmosphere, *Environ. Sci. Technol*. 28:1375–1388

Streibel, T., Weh, J., Mitschke, S., and Zimmermann, R. (2006). Thermal Desorption/Pyrolysis Coupled with Photoionization Time-of-Flight Mass Spectrometer for the Analysis of Molecular Organic Compounds and Oligomeric and Polymeric Fractions in Urban Particulate Matter, *Anal. Chem*. 78(15):5354–5361.

Sykes, D. C, Woods III, E., Smith, G. D., Baer, T., and Miller, R. E. (2002). Thermal Vaporization-Vacuum Ultraviolet Laser Ionization Time-of-Flight Mass Spectrometer of Single Aerosol Particles, *Anal. Chem*. 74:2048–2053.

Watson, J. G. (2002). Visibility: Science and Regulation, *J. Air Waste Man. Assoc*. 52:628–713.

Wilson, K. R., Jimenez-Cruz, M., Nicholas, C., Belau, L., Leone, S. R., and Ahmed, M. (2006). Thermal Vaporization of Biological Nanoparticles: Fragment-Free VUV Photoionization Mass Spectra of Tryptophan, Phenylalanine-Glycine-Clycine and B-carotene, Submitted to *J. Phys. Chem. A* 110:2106–2113.

Woods, III, E., Smith, G. D., Dessiaterik, Y., Baer, T., and Miller, R. E. (2001). Quantitative Detection of Aromatic Compounds in Single Aerosol Particle Mass Spectrometry, *Anal. Chem*. 73:2317–2322.

Zhang, Q., Alfarra, M. R., Worsnop, D. R., Allan, J. D., Coe, H., Canagaratna, M. R., and Jimenez, J. L. (2005). Deconvolution and Quantification of Hydrocarbon-Like and Oxygenated Organic Aerosols Based on Aerosol Mass Spectrometry, *Environ. Sci. Technol*. 39:4938–4952.

Zhang, X., Smith, K. A., Worsnop, D. R., Jimenez, J., Jayne, J. T., and Kolb, C. E. (2002). A Numerical Characterization of Particle Beam Collimation by an Aerodynamic Lens-Nozzle System: Part 1. An Individual Lens or Nozzle, *Aerosol Sci. Technol*. 36:617–631.